

Spontaneous, Solvent-Free, Polymer-Templated, Solid–Solid Transformation of Thin Metal Films into Nanoparticles

Olivia Hernández-Cruz,[†] Lizeth Avila-Gutierrez,[†] Mikhail G. Zolotukhin,^{*,†} Gonzalo Gonzalez,[†] B. Marel Monroy,[†] Raúl Montiel,[‡] Ricardo Vera-Graziano,[†] Josue E. Romero-Ibarra,[†] Omar Novelo-Peralta,[†] and Felipe Alonso Massó Rojas[§]

[†]Instituto de Investigaciones en Materiales, Universidad Nacional Autónoma de México, Apartado Postal 70-360, CU, Coyoacán, 04510, Ciudad de México, D.F., México

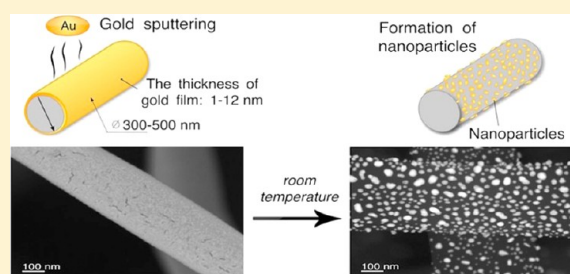
[‡]Universidad Autónoma Metropolitana, México, San Rafael Atlixco 186, Vicentina, Iztapalapa, 09340 Ciudad de México, D.F., México

[§]Instituto Nacional de Cardiología “Ignacio Chávez”, Juan Badiano 1 Col Sección XVI Tlalpan C.P., 14080 Ciudad de México, D.F., México

S Supporting Information

ABSTRACT: Metal nanoparticles have unusual optical, electronic, sensing, recognition, catalytic, and therapeutic properties. They are expected to form the basis of many of the technological and biological innovations of this century. A prerequisite for future applications using nanoparticles as functional entities is control of the shape, size, and homogeneity of these nanoparticles and of their interparticle spacing and arrangement on surfaces, between electrodes, or in devices. Here, we demonstrate that thin films of gold, silver, and copper sputter-deposited onto the surface of an organic polymer poly[[1,1':4',1''-terphenyl]-4,4''-diyl(2-bromo-1-carboxyethylidene)] (PTBC) undergo spontaneous solid–solid transformation into nanoparticles. Furthermore, we show that, by varying the thickness of the films, the volume-to-surface ratio of the polymer substrate, and the amount of plasticizer, it is possible to control the rate of transformation and the morphology of the nanoparticles formed. PTBC containing Au nanoparticles was found to enhance the cell adhesion and proliferation. To the best of our knowledge, our findings constitute the first experimental evidence of spontaneous, room-temperature, solid–solid transformation of metal films sputtered onto the surface of an organic polymeric substrate into nanoparticles (crystals).

KEYWORDS: Metal nanoparticles, polymer template, electrospinning, spontaneous transformation, dewetting, Ostwald ripening



The development of novel structures on the nanometer scale has been one of the most significant achievements in materials science over the last 10–15 years. Metal nanoparticles (NP, sometimes called nanoclusters) and, particularly, gold (AuNP) and silver (AgNP) nanoparticles have received ever-increasing research attention. Interest in NP has risen exponentially in the past two decades, and several complementary reviews on nanoparticles have appeared documenting the importance of this area of nanoscience.^{1–10}

Gold nanoparticles can be created in a variety of different shapes and sizes using different synthetic strategies, among which the most common is reduction of a gold(III) compound in the presence of a stabilizing ligand, such as a thiol, disulfide, or amine. The reduction of auric acid in water using citrate, which also serves as a stabilizing ligand, is a particularly common method. Stabilization of AuNP by surfactants or protection by a shell of thiolate ligands make AuNP more refractory toward aggregation and other modes of decay, thus enabling the isolation of AuNP of different sizes and exploration of their size-dependent properties. Many protocols

using various solvents, ligands, and reducing agents, and sometimes further additives, have been presented.

Similarly, the chemical synthesis of AgNPs in solution usually employs the following three main components: (1) metal precursors, (2) reducing agents and (3) stabilizing/capping agents. A common feature of the methods is that a stabilizer (or dispersant), often an organic compound, is employed during the synthesis. However, the stabilizer, which prevents both the direct apposition of NPs and their growth, is difficult to remove after synthesis.

Ideally, an efficient method of NP preparation should exclude the presence of reduction agents and stabilizers. At the same time, to optimize and extend the applications of NP, it is desirable to control both the distance between the particles and their size. Finally, their integration onto surfaces and their accessibility on various templates (including materials of high

Received: May 2, 2016

Revised: August 10, 2016

Published: August 23, 2016

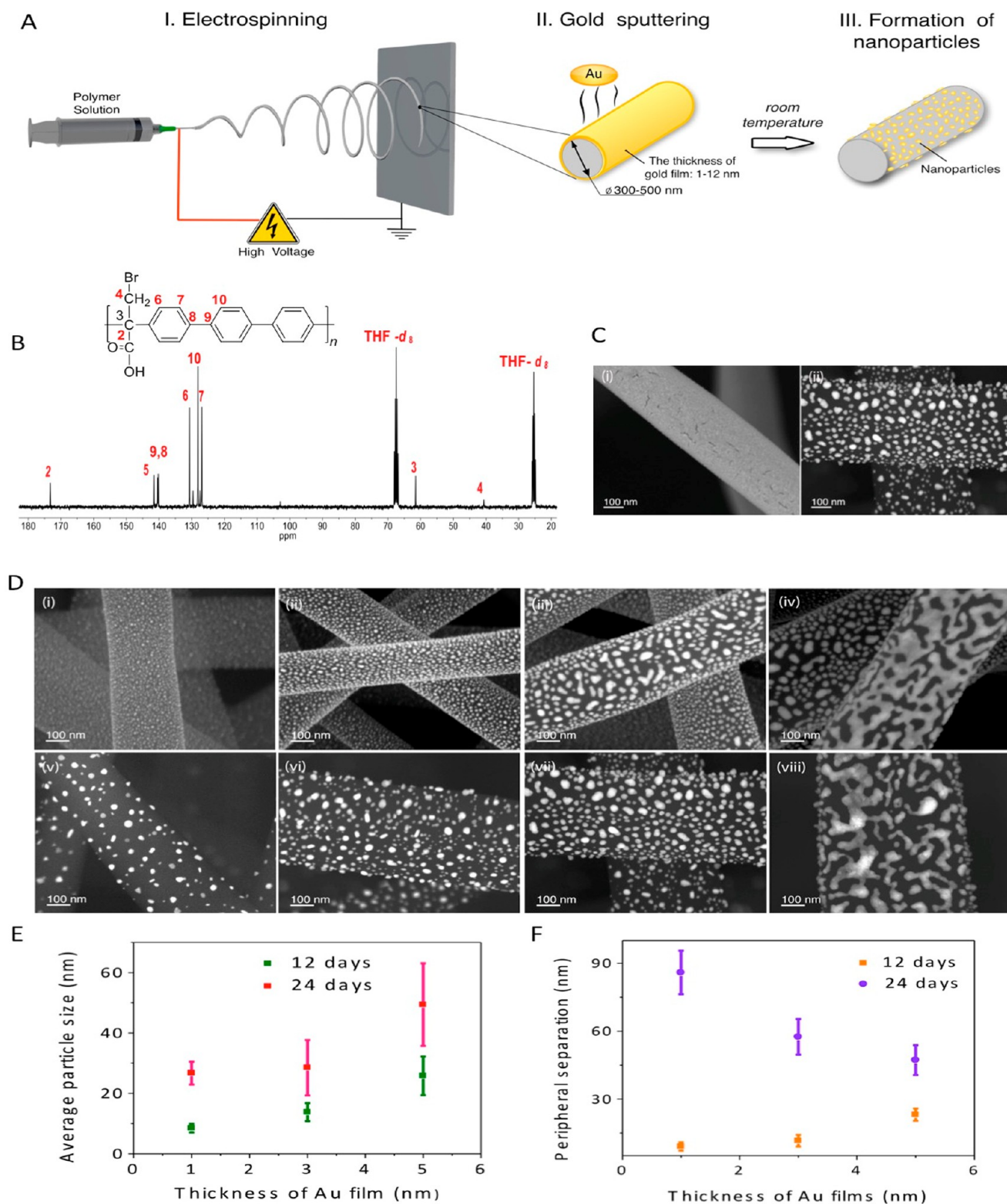


Figure 1. (A) Scanning electron microscope images of PTBC fibers and nanocomposites. (A) Schematic of the nanocomposite formation. (B) ^{13}C NMR (solution in $\text{THF-}d_8$) spectrum of polymer PTBC. (C) SEM images taken immediately after fabrication of the fibers and gold sputtering (i) and 2 weeks later (ii). (D) SEM images showing the development of the Au nanoparticles from gold sputtered films of different thicknesses taken at 12 (i–iv) and 26 days (v–viii). The thicknesses of the films for (i–iv) and (v–viii) were as 1, 3, 5, and 10 nm, respectively. (E) Particle size and (F) particle–particle spacing as a function of post-deposition time (average size of particles and average distance of the edge of a particle to the edge of its nearest neighbor were measured from the SEM images).

surface area) is in practice a prerequisite for exploiting the properties of AuNP and AgNP for a variety of applications.

In this context, polymer-based nanocomposites present a promising challenge. Polymers can easily be processed to form

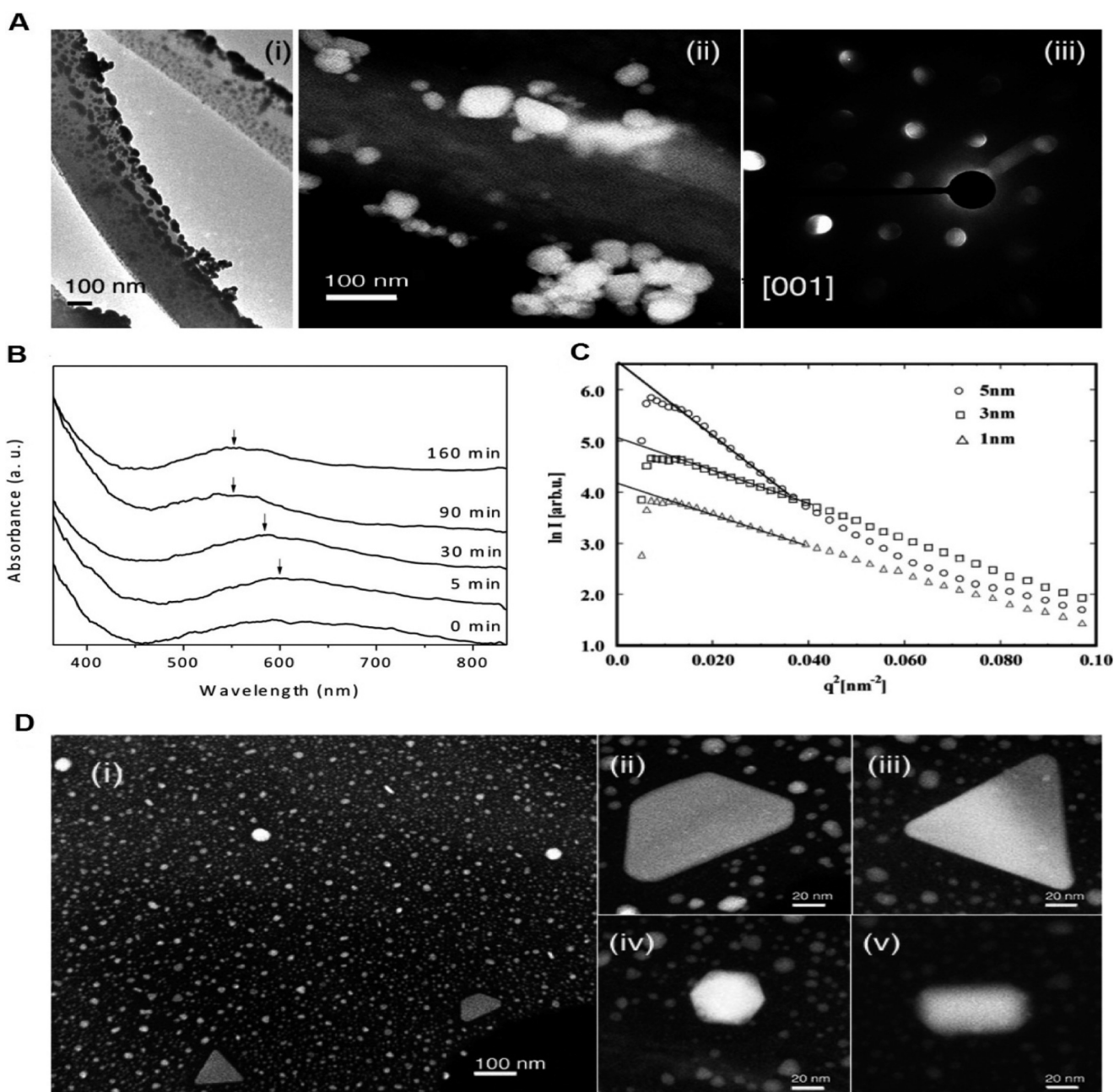


Figure 2. Electron microscopy, UV-, and X-ray characterization of the nanoparticles. (A) TEM bright field (i), STEM dark field (ii), and convergent beam electron diffraction (CBED) pattern of nanofibers 2 weeks after sputtering of 3 nm gold film (iii). (B) UV-visible range absorption spectra of the dried nanofibers after gold sputtering. (C) Fits of SAXS data to the Guinier equation. The values of R_g obtained from the slope of this plot using the SAXS fit software package. (D) STEM images of gold nanoparticles formed onto PTBC film (i–v).

templates for nanoparticles. A straightforward, cheap and unique method in which polymer fibers with a diameter in the range of from less than 10 nm to over 1 μm are formed is provided by electrospinning of polymer solutions in the presence of an intense electric field (typically 10^5 – 10^6 V m^{-1}) which is applied between the spinneret and a conductive collector.^{11–13} The reduction of diameter into the nanometer range gives rise to a set of favorable properties including an extremely high surface-to-volume ratio, variations in wetting behavior, and modification of the release rate. Electrospinning of nanofibers is a very flexible method, which allows for the manufacture of long nanofibers and provides a relatively easy route for their assembly and manipulation. Nanofibers have

been produced by electrospinning many different polymers of various compositions.

Here, we demonstrate a new approach to nanocomposites based on the previously unknown phenomenon of conversion of metal films (gold, silver, and copper) sputtered onto nanofibers of an organic polymer poly[[1,1':4',1''-terphenyl]-4,4''-diyl(2-bromo-1-carboxyethylidene)] (PTBC) into nanoparticles (Figure 1A). Furthermore, we show that, by varying the thickness of the gold film, the time after deposition, and the amount of the plasticizer, it is possible to control the size of and separation between the particles. To the best of our knowledge, our findings constitute the first experimental evidence of room

temperature spontaneous transformation of metal films to nanoparticles on the surface of an organic polymeric substrate.

PTBC was obtained by metal-free, room-temperature, superacid-catalyzed step-growth polymerization of terphenyl with 3-bromopyruvic acid in the presence of the Bronsted superacid $\text{CF}_3\text{SO}_3\text{H}$ (TFSA) according to the method published.¹⁴ The polymer obtained after isolation from the reaction medium, then washed and dried, has the appearance of a white fiber-like powder and exhibits good solubility in aprotic solvents. Transparent strong flexible films could be cast from the polymer solutions. The inherent viscosity of a 0.2% polymer solution in tetrahydrofuran (THF) at 25 °C measured in an Ubbelohde viscometer was found to be 0.32 dL/g.

The high solubility of the polymer allowed us reliably to perform spectral studies to delineate its chemical structure, which was confirmed by NMR spectroscopy (Figure 1B). Thermogravimetric analysis of PTBC showed two-step decomposition (with onsets of decomposition at 175 and 325 °C, respectively). DSC analysis did not reveal a glass transition temperature below the decomposition temperatures. The polymer was electrospun to form nanofibers, and gold was sputter-deposited onto these nanofibers to enable SEM measurements. Figure 1C (i) shows an SEM image of a rather typical pattern of randomly oriented circular fibers. After the measurements, the sample of nanofibers was stored in a drawer in the laboratory table. After 2 weeks, we noticed that the sample had developed a slightly reddish color. Intrigued by this observation, we decided to repeat the SEM measurements on the nanofibers as thus altered, i.e., without additional gold sputtering. The SEM image of the altered sample was very different, revealing mostly rather uniformly distributed bright spots (seemingly gold nanoparticles, instead of gold film, as in Figure 1C (ii)).

It is to be noted that this phenomenon was fully reproducible using various different batches of PTBC. It is clear that the formation of the nanoparticles cannot be explained by trivial stripping of the gold film, as will also be confirmed by the results of further studies presented below. In order to reveal the effect of film thickness on the morphological evolution of these gold particles, 1, 3, 5, and 10 nm thick gold films were deposited onto polymeric nanofibers (Figure 1D–F).

In all cases, their self-assembly progressed through an approximately 4 week period, during which the average particle size increased with increasing time after deposition, probably because of coalescence effect. At the same time, the average distance between the edge of a particle and the edge of its nearest neighbor also increased. The greater the thickness of the initial Au film, the less difference there was between AuNP formed within 2 and at 4 weeks (Figure 1E–F). Deposition of a 10 nm gold film leads to the formation of a discontinuous island-like film. TEM bright field and STEM dark field images (Figure 2A ((i) and (ii), respectively)) reveal that particles (which are seen as bright spots in SEM images) consist of aggregates (clusters) of smaller particles of regular shape. Convergent beam electron diffraction (CBED) confirms the crystalline nature of these particles ranged from 10 to 50 nm (Figure 2A (iii)).

It is important that SEM pictures of the samples taken in one (!) year did not reveal any essential changes. It is worthy of note that usually nanofibers produced by electrospinning are used “as obtained” under assumption that all (or almost all) solvent was removed during fiber formation. It seemed plausible that nanofibers would contain negligible amounts of

residual solvents (THF and cyclohexanone). However, both nanofibers “as obtained” and after gold sputtering exhibited 6% weight loss until decomposition temperature (175 °C). Residual solvents were removed by drying overnight at 80 °C under vacuum. Remarkably, transformation of gold film into nanoparticles on the surface of dried polymer proceeded very fast, within 1.5–2 h. The residual solvent can be considered as a plasticizer favoring macromolecular mobility and reorganization. At the same time, plasticizer should decrease the proportion of macromolecules on the surface of the polymer thereby affecting surface properties. Although the origin of this effect is not clear, plasticization of the polymer presents a simple and efficient way to control the transformation rate.

The formation of gold nanoparticles is also confirmed by measurements of optical extinction as a function of wavelength. It is well-known that small metallic particles exhibit optical absorption in the ultraviolet–visible region due to the excitation of free electrons in their surfaces (surface plasmon resonance, SPR). The measured UV–visible absorption spectra of the nanofibers after sputtering are shown in Figure 2B. The peaks of the three spectra were normalized to unity. A broad peak at around 700 nm corresponds to absorption of gold film “as sputtered” onto nanofibers. Within 2 h, a new peak at 550 nm has developed, pointing to the formation of gold nanoparticles.

Additional evidence of the formation of gold nanoparticles can be obtained from SAXS measurements using Xeus high-resolution small-angle X-ray scattering (SAXS) equipment. In that case gold nanoparticles were obtained by transformations of thin gold films of measured thicknesses of 1, 3, and 5 nm, fabricated via sputtering. Figure 2C presents the SAXS curves of gold nanoparticles on the surface of polymer templates.

The SAXS data are consistent with others reported in the literature.¹⁵ On the basis of fits of the SAXS data to the Guinier equation, the gyration radii (R_g) characterizing the systems studied were determined. For the samples with the thicknesses of 1, 3, and 5 nm for the gold films, the gyration radii (R_g) of the nanoparticles formed were found to be 9.76 ± 0.18 , 9.84 ± 0.32 , and 15.28 ± 0.15 nm, respectively.

We have also used X-ray diffraction techniques to determine whether the amount of Au on the surface of polymer stays constant after transformation into particles. According to XRD measurements taken on a continuous film and the final nanostructured layer (Figure S1 in the Supporting Information), we conclude that the same gold content exists in the both examined samples; no essential intensity changes were seen in the diffractograms, in sharp contrast with changes in morphology revealed by SEM (Figure 1C (ii)).

It is known that electrospun fibers are electrostatically charged during electrospinning and the charge can remain on the fibers, thereby potentially affecting the process of gold nanoparticle formation. However, the formation of gold nanoparticles is also observed when gold is sputtered onto polymer film obtained by the usual spin-casting technique. Interestingly, in this case, many of the nanoparticles appear with various definite forms such as hexahedra, decahedra, and bipyramids, as well as triangular plates and rods (Figure 2D), while in the former they are more or less rounded globules. Thus, overall, the experimental results unambiguously demonstrate the spontaneous transformation of gold film sputtered onto either polymer nanofibers or films into nanoparticles self-assembled as clusters (on nanofibers) or rather uniformly dispersed, crystalline formations (on films).

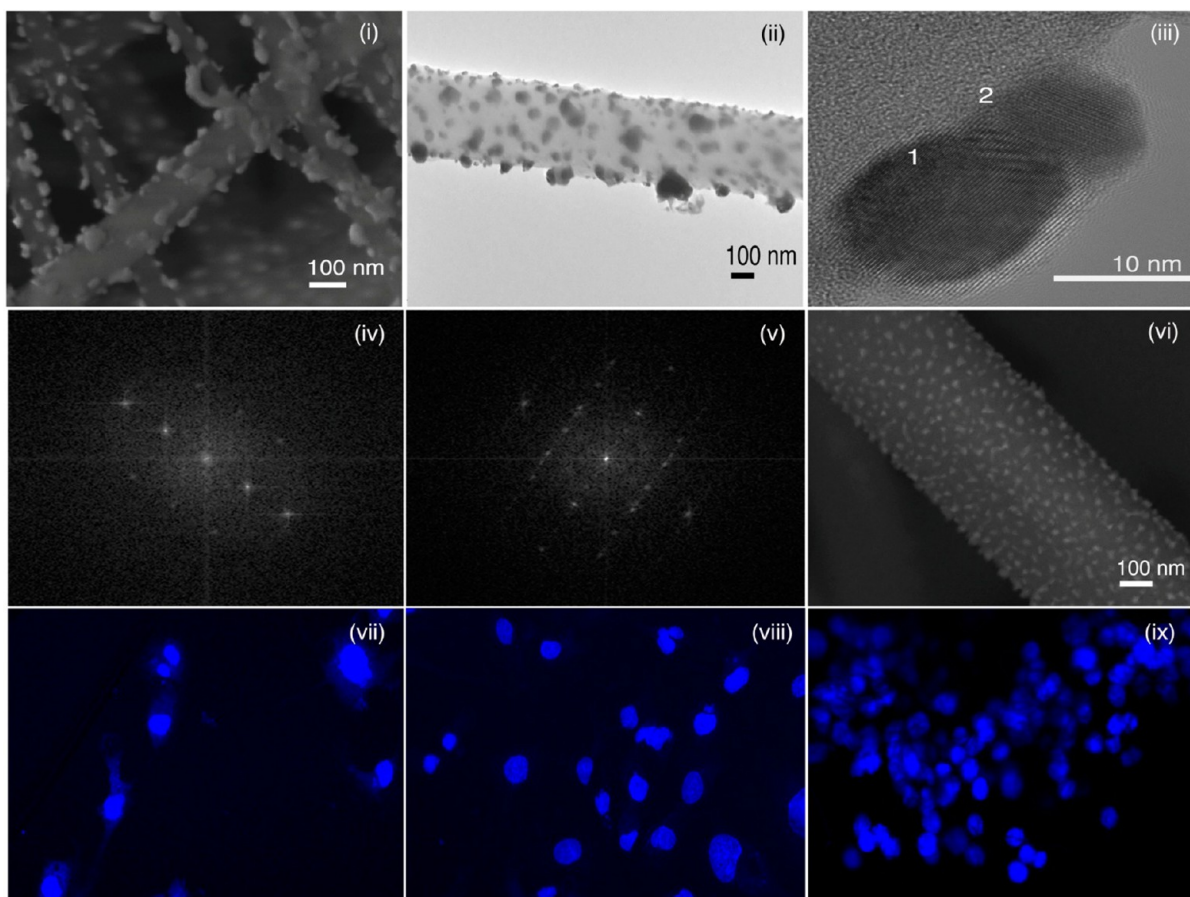


Figure 3. SEM and TEM images of Ag and Cu nanoparticles, confocal images of Jurkat cells adhered on PTBC nanofibers. SEM images of nanoparticles of silver (i) and copper (vi). TEM image of silver nanoparticles (ii); HRTEM images of silver nanoparticles (iii) and their fast Fourier transformation (FFT) patterns (iv–v). Confocal images of Jurkat cells adhered on PTBC nanofibers without AuNP (vii) and containing AuNP obtained from 3 (viii) and 5 (ix) nm gold films, respectively.

The characteristics of the gold nanoparticles are generally similar to that of AuNP obtained by chemical reduction.

To address the generality of the process, we have investigated other metals also. Similar to gold, silver sputter-deposited onto nanofibers of dried PTBC is transformed into nanoparticles (Figure 3 (i–ii)), some of which show coalescence (Figure 3 (iii)). Fast Fourier transformation (FFT) patterns from HRTEM images demonstrate the clearly crystalline nature of these nanoparticles (Figure 3 (iv–v)).

To establish whether or not the phenomenon is more general, copper was also sputter-deposited onto PTBC fibers. Figure 3 (vi) shows an SEM image revealing mostly rather uniformly distributed bright spots of a rather typical pattern of randomly oriented circular fibers covered by nanoparticles.

On the whole, this process is different from such well-known phenomena as (1) redeposition and agglomeration of continuous thin metallic films on insulating oxide surfaces after high temperature annealing,^{16,17} (2) migration–coalescence of nanoparticles during deposition of Au, Ag, Cu, or GaAs on amorphous SiO₂ followed by focused ion-beam bombardment,¹⁸ (3) evaporation/condensation, (4) arc-discharge, (5) laser ablation of metallic bulk materials, and (6) the formation of self-assembled gold island arrays on copolymers with microphase–separation structures after the sputtering of gold and annealing.^{19,20}

Although the detailed mechanism of this complex phenomena described is in question, the following factors seem likely to

contribute: the chemical composition of the polymer, the presence of plasticizer, contact and longer-range van der Waals interactions, solid state dewetting, film–surface interfacial energy, surface tensions, and Ostwald ripening. It is very likely that a key factor is the chemical structure of PTBC. This new multifunctional polymer contains various functionalities, such as terphenyl, bromomethyl, and carboxy groups. An interplay of these functional groups results in the surface structure favorable for spontaneous film–particle transformation.

The whole process is driven by surface energy minimization. According to SEM and TEM images, at the early stages of transformation, solid–solid state dewetting takes place. Dewetting of metallic films on a substrate is driven by the reduction of the surface energy of the thin film and of the interface energy between the film and the substrate.^{21,22} As a result, a thin metal film on a polymer surface rearranges itself into an ensemble of separated objects. At a later stage, molecules detach from smaller droplets (with higher surface energy), diffuse on the surface, and finally are incorporated into larger droplets (with lower surface energy) by a mechanism like Ostwald ripening.^{23–25}

It is known that nanostructured surfaces can affect cell–material interactions such as cell adhesion, proliferation, and differentiation.²⁶ To explore the interaction between cells and PTBC nanofibers containing gold nanoparticles, Jurkat cells were seeded in RPMI 1640 medium in the presence of two types of PTBC nanofibers—those with coatings of gold

nanoparticles and those without (see Methods in [Supporting Information](#)). Adhesion of Jurkat cells was negligible to nanofibers without gold nanoparticles. Nanofibers containing gold nanoparticles obtained from 1 nm gold film showed no significant cell adhesion, whereas for the samples with AuNP obtained from 3 and 5 nm gold film the cell adhesion capability increased progressively ([Figure 3](#) (vii-ix)).

In summary, we have demonstrated, for the first time, spontaneous, solvent-free, room-temperature, polymer-templated, solid–solid transformation of thin films of gold, silver, and copper into nanoparticles on the surface of a functional organic polymer (PTBC). Gold film sputtered onto flat polymer film transforms into highly ordered crystalline structures, while gold and silver sputtering onto nanofibers favors the formation of nanoparticle clusters. These transformations proceed when the thickness of the sputtered gold film does not exceed 12–15 nm. It is important that this solvent-free, solid–solid transformation process affords fully accessible nanoparticles, even in such high surface-to-volume materials as nanofibers, which is a particularly important advantage in regard to their availability for sensor, biomedical, and catalytic applications. The whole process is essentially simpler in comparison with previously known chemical- and physical-based methods for the formation of metal nanoparticles.

The technology based on the transformation of thin metal films into polymer-supported nanoparticles offers the following advantages: (1) exceptional purity of the metal nanoparticles (as a matter of fact, the nanoparticles are crystals), (2) control of shape, size, and interparticle spacing, (3) the nanoparticles formed are free of residual chemicals (precursors, stabilizers, reducing agents, etc.), (4) ability to control the rate of the transformation using plasticization of the polymer matrix: use of nonplasticized polymer affords full transformation within 1.5–2 h, while polymer plasticization slows down the rate of transformation, (5) full accessibility of the nanoparticles, (6) the large size and long-term stability of polymer-supported nanoparticle samples, (7) easy scaling-up of the process of nanoparticle formation by application of large capacity metal sputtering equipment, (8) easy handling (manipulation) of polymer-supported nanoparticles.

While this work was focused only on gold, silver, and copper, similar behavior is expected also for other metals thereby opening up exciting opportunities for the construction of various complex nanostructures with tailored functionalities. The emerging understanding of the mechanism of this multiaspect transformation promises to allow the design of new applications utilizing the morphology of these novel materials.

■ ASSOCIATED CONTENT

Supporting Information

The Supporting Information is available free of charge on the ACS Publications website at DOI: [10.1021/acs.nanolett.6b01780](https://doi.org/10.1021/acs.nanolett.6b01780).

Methods and characterization and Figure S1 ([PDF](#))

■ AUTHOR INFORMATION

Corresponding Author

*E-mail: zolutukhin@iim.unam.mx.

Notes

The authors declare no competing financial interest.

■ ACKNOWLEDGMENTS

The authors acknowledge the financial support from CONACYT Mexico (Grants 151842 and 251693) and from DGAPA-UNAM (PAPIIT IN 105314-3). Thanks are due to Dr. A. Paez Arenas of National Institute of Cardiology for evaluation of the cell adhesion and proliferation in PTBC fibers with nanoparticles; E. R. Morales, S. Morales, A. Lopez Vivas, and P. Castillo for assistance with thermal and spectroscopic analysis. The editorial assistance of Dr. Robert E. Dale is much appreciated.

■ REFERENCES

- (1) Templeton, A. C.; Wuelfing, W. P.; Murray, R. W. *Acc. Chem. Res.* **2000**, *33*, 27–36.
- (2) Daniel, M. C.; Astruc, D. *Chem. Rev.* **2004**, *104*, 293–346.
- (3) Rao, C. N. R.; Cheetham, A. K., Eds. *The Chemistry of Nanomaterials: Synthesis, Properties and Applications*, Vol. 1 and 2; Wiley-VCH: Weinheim, Germany, 2004.
- (4) Jennings, T.; Strouse, G. *Adv. Exp. Med. Biol.* **2007**, *620*, 34–47.
- (5) Murray, R. W. *Chem. Rev.* **2008**, *108*, 2688–2720.
- (6) Sardar, R.; Funston, A. M.; Mulvaney, P.; Murray, R. W. *Langmuir* **2009**, *25*, 13840–13851.
- (7) Giljohann, D. A.; Seferos, D. S.; Daniel, W. L.; Massich, M. D.; Patel, P. C.; Mirkin, C. A. *Angew. Chem., Int. Ed.* **2010**, *49*, 3280–3294.
- (8) Dreaden, E. C.; Alkilany, A. M.; Huang, X.; Murphy, C. J.; El-Sayed, M. A. *Chem. Soc. Rev.* **2012**, *41*, 2740–2779.
- (9) Zhao, P.; Li, N.; Astruc, D. *Coord. Chem. Rev.* **2013**, *257*, 638–665.
- (10) Wang, C.; Astruc, D. *Chem. Soc. Rev.* **2014**, *43*, 7188–7216.
- (11) Ramakrishna, S.; Fujihara, K.; Teo, W. E.; Lim, T. C.; Ma, Z. *Electrospinning and nanofibers*; World Scientific: Singapore, 2005.
- (12) Wendorf, J. H.; Agarwal, S.; Greiner, A. *Electrospinning*; Wiley-VCH: Singapore, 2012.
- (13) Gómez-Pachón, E. Y.; Sánchez-Arévalo, F. M.; Sabina, F. J.; Maciel-Cerda, A.; Campos, R. M.; Batina, N.; Morales-Reyes, I.; Vera-Graziano, R. *J. Mater. Sci.* **2013**, *48*, 8308–8319.
- (14) Hernández-Cruz, O.; Zolotukhin, M. G.; Fomine, S.; Alexandrova, L.; Aguilar-Lugo, C.; Ruiz-Treviño, A.; Ramos-Ortiz, G.; Maldonado, J. L.; Cadenas-Pliego, G. *Macromolecules* **2015**, *48*, 1026–1037.
- (15) Polte, J.; Ahner, T. T.; Delissen, F.; Sokolov, S.; Emmerling, F.; Thunemann, A. F.; Kraehnert, R. *J. Am. Chem. Soc.* **2010**, *132*, 1296–1301.
- (16) Kwon, J.-Y.; Yoon, T.-S.; Kim, K.-B.; Min, S.-H. *J. Appl. Phys.* **2003**, *93*, 3270–3278.
- (17) Gadkari, P. R.; Warren, A. P.; Todt, R. M.; Petrova, V.; Coffey, K. R. *J. Vac. Sci. Technol., A* **2005**, *23*, 1152–1161.
- (18) Shirakawa, H.; Komiyama, H. *J. Nanopart. Res.* **1999**, *1*, 17–30.
- (19) Metwalli, E.; Couet, S.; Schlage, K.; Rohlsberger, R.; Korstgens, V.; Ruderer, M.; Wang, W.; Kaune, G.; Roth, S. V.; Muller-Buschbaum, P. *Langmuir* **2008**, *24*, 4265–4272.
- (20) Morkved, T. L.; Wiltzius, P.; Jaeger, H. M.; Grier, D. G.; Witten, T. A. *Appl. Phys. Lett.* **1994**, *64*, 422–422.
- (21) Gentili, D.; Foschi, G.; Valle, F.; Cavallini, M.; Biscarini, F. *Chem. Soc. Rev.* **2012**, *41*, 4430–4443.
- (22) Thompson, C. V. *Annu. Rev. Mater. Res.* **2012**, *42*, 399–434.
- (23) Ostwald, W. Z. *Physikalische Chemie* **1897**, *22*, 289–330.
- (24) Wagner, C. Z. *Electrochimie* **1961**, *65*, 581–591.
- (25) Baldan, A. *J. Mater. Sci.* **2002**, *37*, 2171–2202.
- (26) Stevens, M. M.; George, J. H. *Science* **2005**, *310*, 1135–1138.